

AN EQUATION-FREE, MULTISCALE APPROACH TO UNCERTAINTY QUANTIFICATION

The authors' equation- and Galerkin-free computational approach to uncertainty quantification for dynamical systems conducts UQ computations using short bursts of appropriately initialized ensembles of simulations. Their basic procedure estimates the quantities arising in stochastic Galerkin computations.

Recently, interest has grown in developing efficient computational methods (both sampling and nonsampling) for studying ordinary or partial differential equations (ODEs or PDEs) with random inputs. Stochastic Galerkin (SG) methods based on generalized polynomial chaos (gPC) representations have several appealing features (see the sidebar). However, when the model equations are complicated, the numerical implementation of SG or gPC algorithms can become highly nontrivial, and we must take care to design robust and efficient solvers for the resulting systems of equations.

We propose an equation-free, multiscale computational approach to uncertainty quantification (UQ) that, in some sense, combines sampling methods with nonsampling ones. This approach uses short bursts of appropriately initialized sampling runs to estimate quantities arising in SG numerics, circumventing the need to derive equations for gPC coefficients through the SG procedure.

Equation-Free Computation

The equation-free approach¹⁻³ has been designed specifically for problems that are “effectively simple”—that is, problems for which we believe macroscopic (averaged, population-level, coarse-grained, effective) evolution equations exist conceptually, although they aren't available in closed form. For such problems, the only available model is a fine-scale (atomistic, stochastic, agent-based) simulator, but running this over macroscopic space and time scales is often prohibitively expensive. Our equation-free approach uses the fine-scale simulator as an experiment that can be initialized and run at will.

We want to operate on two levels: first, we design and execute appropriately initialized short-time numerical experiments with the best-available microscopic model. Then, we use these computations' results to estimate the coarse quantities (for example, residuals or action of Jacobians) required to compute with the unavailable macroscopic equations.^{1,2} Thus, to solve the unavailable macroscopic equations, we estimate closures numerically on demand, instead of deriving them analytically. To perform numerical analysis tasks (such as integration, solution of linear and nonlinear equations, and eigen analysis) we act on the microscopic simulation directly (equation-free), taking extensive advantage of matrix-free iterative linear algebra.⁴

We've applied our framework to a variety of problems, from bifurcation analysis of complex sys-

1521-9615/05/\$20.00 © 2005 IEEE
Copublished by the IEEE CS and the AIP

DONGBIN XIU AND IOANNIS G. KEVREKIDIS

Princeton University

ROGER GHANEM

University of Southern California

Approaches to Uncertainty Quantification

Sources of uncertainty generally include those in system parameters as well as in boundary and initial conditions; these are ubiquitous in engineering applications and are often modeled as random variables or processes. Traditional approaches to uncertainty quantification (UQ) include the Monte Carlo method and its variants—for example, Latin Hypercube Sampling¹—which generate ensembles of random realizations for the prescribed random inputs and use repetitive deterministic solvers for each realization. Such methods' convergence rates can be relatively slow, and researchers have devoted extensive time to developing nonsampling methods that employ no repetitive deterministic solvers. These include perturbation methods² and second-moment analysis,^{3,4} which are both well suited for systems with relatively small random inputs and outputs.

The recently developed stochastic Galerkin (SG) methods can exhibit faster convergence for problems with relatively large random inputs and outputs. The SG methods' faster convergence is attributed to the use of generalized polynomial chaos (gPC) representations of random processes. Such representations are generalizations of the Wiener-Hermite polynomial chaos expansion,⁵ which others have applied to various problems in mechanics.⁶ The generalizations employ non-Hermite polynomials to improve efficiency for a wider class of random processes and include global polynomial expansions,^{7,8} piecewise polynomial expansions,^{9,10} and wavelet basis expansions.^{11,12} Although SG methods based on gPC can, in general, converge rapidly, the resulting systems of deterministic equations for the gPC coefficients are often large and coupled, thus we must take care to design efficient and robust solvers for them. The form of the resulting equations can become quite complicated when the underlying differential equations have nontrivial and nonlinear forms.¹³ Furthermore, the dimensionality of the discretized SG equations for an

engineering model can be much larger than the dimensionality of the base case deterministic model.

References

1. G.S. Fishman, *Monte Carlo: Concepts, Algorithms, and Applications*, Springer-Verlag, 1996.
2. M. Kleiber and T.D. Hien, *The Stochastic Finite-Element Method*, John Wiley & Sons, 1992.
3. W.K. Liu, T. Belytschko, and A. Mani, "Probabilistic Finite Elements for Nonlinear Structural Dynamics," *Computer Methods in Applied Mechanics and Eng.*, vol. 56, no. 1, 1986, pp. 61–81.
4. W.K. Liu, T. Belytschko, and A. Mani, "Random Field Finite Elements," *Int'l J. Numerical Methods in Eng.*, vol. 23, no. 16, 1986, pp. 1831–1845.
5. N. Wiener, "The Homogeneous Chaos," *Am. J. Mathematics*, vol. 60, 1938, pp. 897–936.
6. R.G. Ghanem and P. Spanos, *Stochastic Finite Elements: A Spectral Approach*, Springer-Verlag, 1991.
7. D. Xiu and G.E. Karniadakis, "Modeling Uncertainty in Steady State Diffusion Problems via Generalized Polynomial Chaos," *Computer Methods in Applied Mechanics and Eng.*, vol. 191, no. 43, 2002, pp. 4927–4948.
8. D. Xiu and G.E. Karniadakis, "The Wiener-Askey Polynomial Chaos for Stochastic Differential Equations," *SIAM J. Scientific Computing*, vol. 24, no. 2, 2002, pp. 619–644.
9. I. Babuška, R. Tempone, and G.E. Zouraris, "Galerkin Finite Element Approximations of Stochastic Elliptic Differential Equations," *SIAM J. Numerical Analysis*, vol. 42, no. 2, 2004, pp. 800–825.
10. M.K. Deb, I. Babuška, and J.T. Oden, "Solution of Stochastic Partial Differential Equations using Galerkin Finite-Element Techniques," *Computer Methods in Applied Mechanics and Eng.*, vol. 190, no. 48, 2001, pp. 6359–6372.
11. O. Le Maitre et al., "Uncertainty Propagation using Wiener-Haar Expansions," *J. Computational Physics*, vol. 197, no. 1, 2004, pp. 28–57.
12. O. Le Maitre et al., "Multiresolution Analysis of Wiener-Type Uncertainty Propagation Schemes," *J. Computational Physics*, vol. 197, no. 2, 2004, pp. 502–531.
13. D. Xiu and S.J. Sherwin, "Uncertainty Modelling in Hyperbolic Systems and its Applications in Reduced Modelling of a Human Arterial Network," to be published in *SIAM J. Scientific Computing*, 2005.

tems to homogenization of random media,^{2,3,5–10} but in this article, we apply our equation-free approach to UQ. Our examples are dynamical systems (ODEs) with random inputs, but we can readily extend our approach to certain types of PDEs.¹¹ In this context, ensembles of short bursts of deterministic ODE simulations through Monte Carlo (MC) sampling act as the detailed, microscopic model; the coarse-grained dynamics are the long-term dynamics of a set of gPC expansion coefficients of the ensemble statistics. The idea is that deterministic equations exist and accurately close

at the level of this leading gPC expansion coefficient set, so these finite degrees of freedom are sufficient for representing the ensemble statistics. The normal procedure for obtaining evolution equations for these leading gPC coefficients would be to perform an SG projection of the governing stochastic equations on the gPC basis; truncating this Galerkin projection gives an approximation of these equations. We project the results of short bursts of MC sampled dynamics onto the gPC basis (thus, the *Galerkin-free* label). We illustrate equation-free projective integration and equation-

free fixed-point and limit-cycle computations for a class of random dynamical systems.

Computational Framework

Consider a nonlinear system of equations

$$\frac{d\mathbf{x}}{dt} = \mathbf{f}(\mathbf{x}), \quad \mathbf{x}(0) \equiv \mathbf{x}_0, \quad (1)$$

where $\mathbf{x} = \mathbf{x}(t) \in \mathbb{R}^n$, $n = 1, 2, \dots$, is a vector-valued function of time, and $\mathbf{f}: U \rightarrow \mathbb{R}^n$ is a smooth function defined on some subset $U \subset \mathbb{R}^n$. In this article, we restrict our exposition to autonomous systems, although we can readily extend our approach to nonautonomous ones.

To represent random inputs, we introduce to Equation 1 a random parameter $\omega \in \Omega$, which belongs to an appropriately defined sample set. For many practical systems—for example, chemical or biological reactions—a major source of uncertainty resides in the parameters associated with material or rate properties. In this article, we study a system of equations for $\mathbf{x}(t, \omega)$,

$$\frac{d\mathbf{x}}{dt} = \mathbf{f}(\mathbf{x}, \omega), \quad \mathbf{x}(0, \omega) = \mathbf{x}_0(\omega), \quad (2)$$

where $\mathbf{f}: U \times \Omega \rightarrow \mathbb{R}^n$, and $\mathbf{x}_0: \Omega \rightarrow \mathbb{R}^n$ is the initial condition. The vector field \mathbf{f} generates a flow $\Phi_t: U \times \Omega \rightarrow \mathbb{R}^n$, which becomes a random vector and satisfies

$$\frac{d}{dt}(\Phi(\mathbf{x}, t; \omega))|_{t=\tau} = \mathbf{f}(\Phi(\mathbf{x}, \tau; \omega)) \quad (3)$$

for all $\mathbf{x} \in U$, $\omega \in \Omega$, and $\tau \in I$, where $I = (a, b) \in \mathbb{R}$ is some interval. A straightforward way to resolve Equation 2 is to use the MC method, wherein we generate multiple realizations of the random inputs for $\omega \in \Omega$ and conduct deterministic simulations for each realization. The results constitute an ensemble of solutions, and we can apply various postprocessing procedures to obtain solution statistics. Generally, we need several realizations to obtain accurate statistics. Hereafter, we refer to MC solutions as fine-scale solutions.

Stochastic Galerkin Approach

gPC expansions provide a way to represent a random solution with fewer degrees of freedom than MC methods. When we use the SG method with a gPC representation, we seek to expand the random solution as

$$\mathbf{x}(t, \omega) = \sum_{m=1}^M \hat{\mathbf{x}}_m(t) \phi_m(\boldsymbol{\xi}(\omega)), \quad (4)$$

where $\{\phi_m\}_{m=1}^M$ is a set of orthogonal polynomial basis functions and $\boldsymbol{\xi}(\omega) = (\xi_1, \dots, \xi_d)$ is a random vector. The dimensionality of the random vector $\boldsymbol{\xi}$, d , is determined by the given random inputs. For instance, d can represent the number of random parameters we intend to model. We can determine these either explicitly through the problem statement or implicitly through an inverse analysis.¹² We determine the total number of the expansion coefficients $\{\hat{\mathbf{x}}_m\}_{m=1}^M$ by d and highest order (p) of the polynomial basis $\{\phi_m\}$ —that is, $M = (d + p)!/d!p!$. Clearly, the problem size for solving UQ grows quickly with d . We determine the expansion coefficients using

$$\hat{\mathbf{x}}_m(t) = \frac{\langle \mathbf{x}(t, \omega) \phi_m(\boldsymbol{\xi}(\omega)) \rangle}{\langle \phi_m^2(\boldsymbol{\xi}(\omega)) \rangle}, \quad m = 1, \dots, M, \quad (5)$$

where $\langle \cdot \rangle$ is the expectation (ensemble average) operator; we can determine the normalization factor $\langle \phi_m^2 \rangle$ analytically prior to any computations once we choose the type of orthogonal polynomials $\{\phi_m\}_{m=1}^M$. For better computational efficiency, we must establish a correspondence between the type of orthogonal polynomial ϕ and the type of random vector $\boldsymbol{\xi}$. These correspondences typically associate a probability density function with the weights of some suitable orthogonal polynomials—for example, Gaussian PDF with Hermite polynomials or uniform PDF with Legendre polynomials.¹³

Equations 4 and 5 define two operations that let us transform between an ensemble of fine-scale solutions $\mathbf{x}(t, \omega)$ and the corresponding expansion coefficients $\{\hat{\mathbf{x}}_m(t)\}$. That is, given an ensemble of solutions $\mathbf{x}(t, \omega)$, we can obtain its expansion coefficients $\{\hat{\mathbf{x}}_m(t)\}$ using Equation 5; conversely, given a set of expansion coefficients $\{\hat{\mathbf{x}}_m(t)\}$, we can use Equation 4 to construct an ensemble of full-scale states $\mathbf{x}(t, \omega)$ by generating a set of random realizations of $\boldsymbol{\xi}(\omega)$. The former operation, in equation-free terminology, is the *restriction*, whereas the latter constitutes a *lifting operator*. We discuss the importance of consistently using random seeds for $\boldsymbol{\xi}(\omega)$ in Equations 4 and 5 elsewhere.¹¹

To obtain evolution equations for the expansion coefficients $\{\hat{\mathbf{x}}_m\}_{m=1}^M$, one conducts the SG projection of Equation 2:

$$\frac{d\hat{\mathbf{x}}_m}{dt} = \hat{\mathbf{f}}_m, \quad \hat{\mathbf{x}}_m(0) = \hat{\mathbf{x}}_{0,m}, \quad m = 1, \dots, M, \quad (6)$$

where $\{\hat{\mathbf{f}}_m\}_{m=1}^M$ and $\{\hat{\mathbf{x}}_{0,m}\}_{m=1}^M$ are the expansion coefficients of \mathbf{f} and \mathbf{x}_0 , respectively. That is,

$$\hat{\mathbf{f}}_m = \frac{1}{\langle \phi_m^2(\xi) \rangle} \left\langle \mathbf{f} \left(\sum_{m=1}^M \hat{\mathbf{x}}_m(t) \phi_m(\xi) \right) \phi_m(\xi) \right\rangle$$

$$\hat{\mathbf{x}}_{0,m} = \frac{\langle \mathbf{x}_0 \phi_m(\xi) \rangle}{\langle \phi_m^2(\xi) \rangle} \quad m = 1, \dots, M. \quad (7)$$

Denoting $\mathbf{y} = (\hat{\mathbf{x}}_1, \dots, \hat{\mathbf{x}}_M)^T$ and $\mathbf{g} = (\hat{\mathbf{f}}_1, \dots, \hat{\mathbf{f}}_M)^T$, we can write the above equation more compactly as

$$\frac{d\mathbf{y}}{dt} = \mathbf{g}(\mathbf{y}), \quad \mathbf{y}(0) = \mathbf{y}_0. \quad (8)$$

Although Equation 8 is a system of deterministic ODEs, for a general nonlinear dynamical system, the analytical form $\mathbf{g}(\mathbf{y})$ can be highly non-trivial to derive and implement; this precise difficulty motivates our equation-free approach.

The Equation-Free Approach

Our equation-free UQ computations don't require the explicit form of $\mathbf{g}(\mathbf{y})$. We now use our approach to integrate the dynamical equations (Equation 8) and present computations of their fixed points and limit cycles.

Coarse-grained projective integration. For dynamical integrations of Equation 8, we follow a general procedure.^{5,14} For a given initial condition $\mathbf{y}^n = \mathbf{y}(t^n)$ at time level $t^n = n\delta t$, $n \geq 1$, where δt is the time step of fine-scale simulators, we take the following steps:

- *Lifting step.* Generate a fine-scale ensemble $\mathbf{x}^n(\omega) = \mathbf{x}(t^n, \omega)$ using the lifting operation in Equation 4.
- *Fine-scale evolution step.* Use $\mathbf{x}^n(\omega)$ as initial conditions and integrate Equation 2 for a short time to obtain $\mathbf{x}^l(\omega) = \Phi(t^l, t^n; \omega)$ for $l > n$ —that is, integrate Equation 2 for $n_f = l - n$ time steps.
- *Restriction step.* Evaluate $\mathbf{y}(t)$ for $t^n \leq t \leq t^l$ using the restriction operation in Equation 5, and estimate numerically $d\mathbf{y}/dt$ at $t = t^l$ (or, more generally, a polynomial approximation of the short \mathbf{y} trajectory). We use this estimate to approximate Equation 8's right-hand side (RHS).
- *Projective integration.* Using \mathbf{y}^l and a local linear model, extrapolate the coarse Equation 8 forward in time using the estimated RHS. We designate the coarse time step to be $\Delta t_c = n_c \delta t$ with $n_c \geq 1$, and we obtain $\mathbf{y}^m = \mathbf{y}(t^m)$, where $t^m = t^l + n_c \delta t = t^n + (n_f + n_c) \delta t$.

This procedure completes an integration of Equation 8 from t^n to t^m with a global time step Δt

$= t^m - t^n$. We repeat the procedure until we reach the prescribed final integration time. Simply using the estimated time derivative for the extrapolation constitutes the projective forward Euler method; others have constructed and discussed more general, multistep, and even implicit forward and backward projective integration methods.^{2,5,14,15}

Fixed-point computation. We can also compute fixed points of the reduced system in Equation 8 through short bursts of dynamic simulation, combining it with matrix-free techniques of iterative linear algebra. Indeed, we can find steady states of Equation 8 as fixed points of its coarse time-stepper

$$\mathbf{y} - \Phi_\tau(\mathbf{y}) = 0, \quad (9)$$

where $\Phi_\tau(\mathbf{y})$ is the result of lifting from \mathbf{y} , evolving the fine-scale computation for time τ and restricting back to \mathbf{y} . Fixed-point algorithms for solving Equation 9, such as the Newton-Raphson method, require the repeated solution of sets of linear equations involving Equation 9's Jacobian. Matrix-free methods (such as Newton-Krylov-GMRES) for solving Equation 9 use function evaluations (coarse time-stepping) with (appropriately chosen) nearby coarse initial conditions to estimate the action of Equation 9's Jacobian (its matrix-vector product with selected vectors) without explicitly evaluating this Jacobian. We can thus “wrap” the solution of linear and nonlinear equations, as well as the eigencomputations that characterize the coarse solutions' linear stability, around existing fine-scale deterministic codes.^{2,15}

Limit-cycle computation. We can find a dynamical system's limit cycle as the solution of a fixed-point problem similar to Equation 9:

$$\mathbf{x} - \Phi_T(\mathbf{x}) = 0,$$

where T is the period of the limit cycle. This is a nonlinear eigenproblem, characterized by a one-parameter infinity of solutions: each point on the limit cycle satisfies this equation for the right period. Solving this equation as a shooting boundary value problem qualitatively corresponds to studying the dynamics in terms of a *Poincaré map*—that is, recording the successive points at which an evolving trajectory crosses transversely a hyperplane in phase space. The limit cycle is found as a fixed point of this Poincaré or return map.

In the presence of uncertainty, we can reasonably consider a coarse-limit cycle of Equation 3 to be

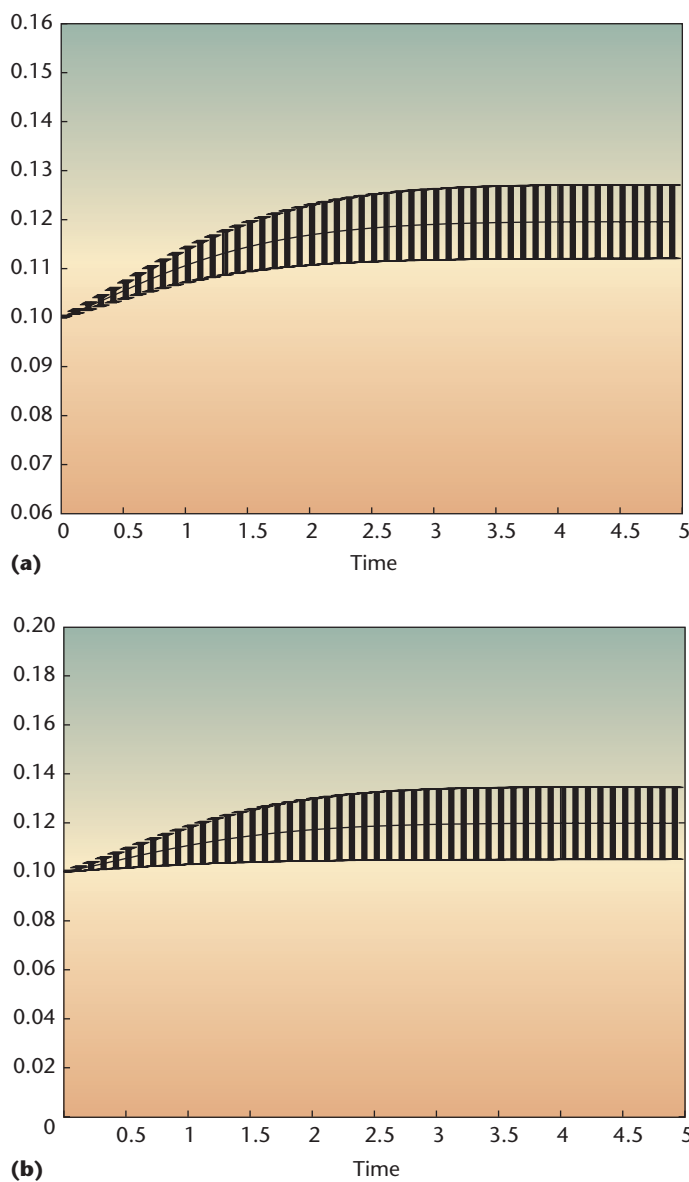


Figure 1. Uncertainty evolution for x_1 in error bars. We show the evolution of the continuous stirred-tank chemical reactor equations using (a) 10 percent uniform uncertainty in the parameter β and (b) 10 percent uniform uncertainty in the Da number. The gaps between the error-bar clusters indicate coarse projective integration steps.

the fixed point of the following coarse Poincaré map: an ensemble of initial conditions on a Poincaré hyperplane, characterized by a set of leading gPC coefficients, which, when evolved forward in time until each one returns to the hyperplane, result in a new ensemble with the same values of leading gPC coefficients. We will also need to determine the gPC coefficients of the ensemble of first return times as part of the process.

Numerical Examples

We employ a continuous stirred-tank chemical reactor (CSTR) with a single, irreversible exothermic reaction as our model problem. The set of two coupled nonlinear ordinary governing equations takes the following form:

$$\frac{dx_1}{dt} = -x_1 + Da \cdot (1 - x_1) \exp\left(\frac{x_2}{1 + x_2 / \gamma}\right) \equiv f_1(x_1, x_2)$$

$$\frac{dx_2}{dt} = -x_2 + B \cdot Da \cdot (1 - x_1) \exp\left(\frac{x_2}{1 + x_2 / \gamma}\right) - \beta(x_2 - x_{2c}) \equiv f_2(x_1, x_2). \quad (10)$$

Here, x_1 is the conversion and x_2 is the dimensionless temperature. A. Uppal, W.H. Ray, and A.B. Poore detail the model's various dimensionless parameters (such as the Damkoehler number Da , heat of reaction B , heat transfer coefficient β , activation energy γ , and coolant temperature x_{2c}) and describe the model's rich nonlinear dynamics.¹⁶ In this article, we fix the parameter $B = 22$ and assume uncertainty in the parameters β or Da .

Dynamical Integrations

In the first test case, we set $B = 22$, $Da = 0.07$, and designate β to be a random variable with 10 percent uncertainty—that is, $\beta = \langle \beta \rangle (1 + \sigma \xi(\omega))$, where $\langle \beta \rangle = 3$, $\sigma = 0.1$, and ξ is a random variable uniformly distributed in $(-1, 1)$. Both the fine-scale solutions and coarse projective integration employ a second-order integrator. Each deterministic integration of the fine-scale model in the MC simulation ensemble has the time step $\delta t = 0.005$; after five such time steps ($n_f = 5$) and the corresponding restrictions, the projective time step for the coarse integrator is $\Delta t_c = 0.025$ (that is, $n_c = 5$). Figure 1a shows in error bars the evolution of the random solution ensemble. At the chosen parameter values, all random solutions approach a steady state, as do the error bars. The gaps between the error-bar clusters indicate the coarse projective integration steps, when the coarse solution jumps (is projected forward in time). Figure 1b shows a similar result, where $\beta = 0.3$ and the uncertainty is in the Damkoehler number $Da = \langle Da \rangle (1 + \sigma \xi)$, where $\langle Da \rangle = 0.07$ and $\sigma = 0.1$.

Figure 2 shows the evolution of x_1 in three-dimensional plots, where one axis shows the range of the random parameter Da , and the time axes are normalized to $(0, 1)$. For the chosen Da ranges, the solution might reach a steady state (Figure 2a), or become periodic (Figure 2b). Again, the solution

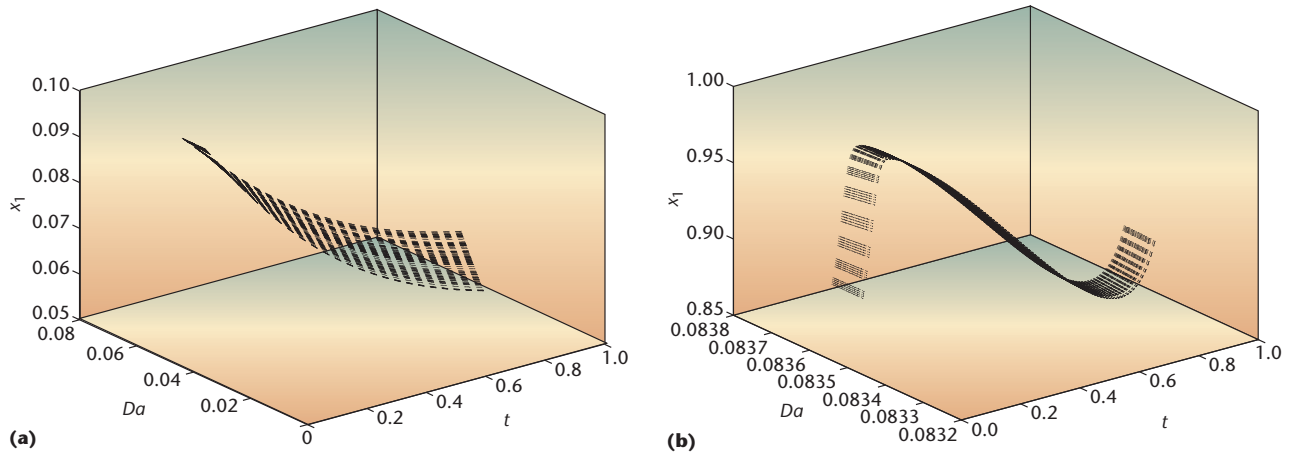


Figure 2. Uncertainty evolution for x_1 in three-dimensional plots. We show (a) the approach to a steady-state computation with 10 percent uniform uncertainty in Da and (b) a limit-cycle computation with 10 percent uniform uncertainty in Da . Coarse integration steps occur in the gaps between the clusters. The time axis is normalized to (0, 1).

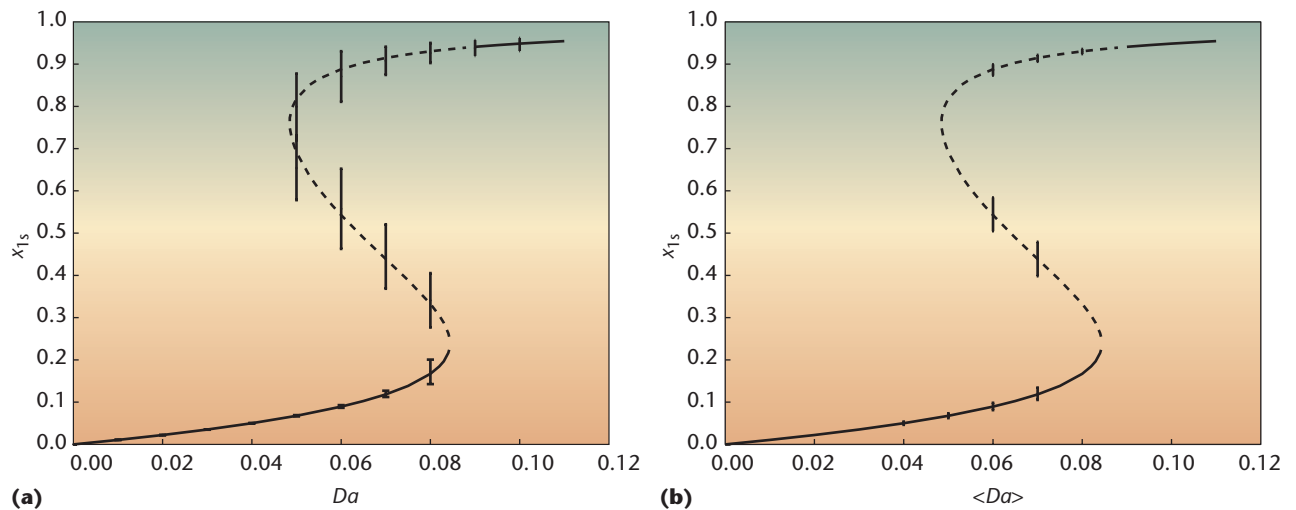


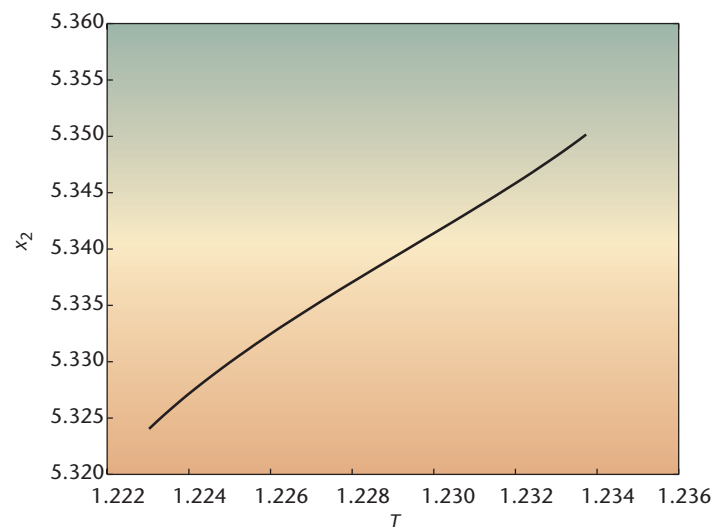
Figure 3. Coarse fixed-point results. Random steady state solutions of x_1 at (a) 10 percent uncertainty in β as a function of Da and (b) 10 percent uncertainty in Da as a function of the average Da .

clusters indicate the fine-scale MC solutions, and coarse projective integration steps occur in the gaps between clusters.

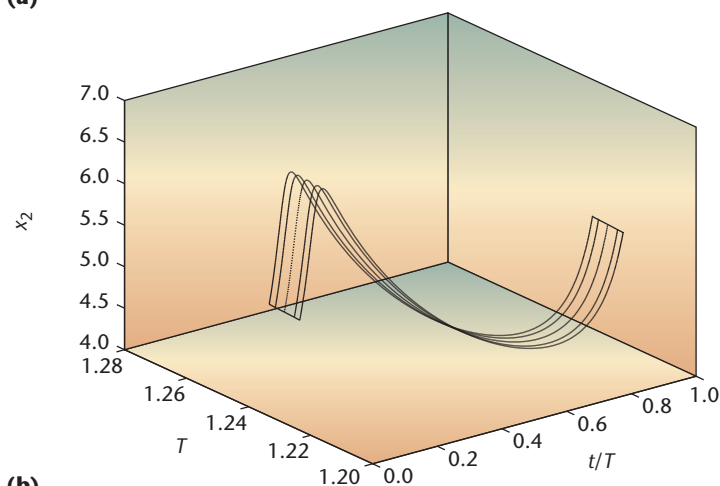
Fixed-Point Calculations

By using a Newton method on Equation 8's coarse time-stepper, we can compute random stable or unstable fixed points. Due to the small number of coarse variables required (overall, on the order of 10 gPC coefficients), we use Newton with numerical derivatives. When the number of coarse variables becomes too large for a detailed estimation of

the Jacobian, we can use matrix-free methods such as NK-GMRES or quasi-Newton methods, such as Broyden. Figure 3a plots the coarse fixed-point results obtained with $B = 22$ and $\beta = \langle\beta\rangle(1 + 0.1\xi(\omega))$, where $\langle\beta\rangle = 3$. We plot the results as a bifurcation diagram with respect to the Da number. The lines denote the deterministic results for the average $\beta = 3$, with the solid line denoting stable fixed points and the dashed line denoting unstable ones. We plot the random solutions at various Da values in error bars; the width of these error bars increases close to the turning points in Da .



(a)



(b)

Figure 4. Oscillations under certainty. Stochastic limit-cycle solution for Equation 10 with $B = 22$, $\beta = 3$, and a uniformly distributed random $Da \sim (0.083, 0.084)$. We show (a) correspondence between random period $T(\omega)$ and $x_2(\omega)$, when $x_1(\omega) = 0.9$ is fixed; (b) several realizations of the periodic solutions.

Figure 3b shows the random fixed points for $B = 22$, $\beta = 3$, and $Da = \langle Da \rangle (1 + 0.1\xi)$ —that is, with 10 percent uncertainty in the Damkoehler number Da . We plot the data as a bifurcation diagram with respect to the average Damkoehler number $\langle Da \rangle$. Again, we denote the deterministic solutions corresponding to $\langle Da \rangle$ with continuous curves and the random solutions with error bars.

We deliberately chose the conditions in regimes where multiplicity occurs for the deterministic problem. Different solution branches for the deterministic problem have their analogs in different stationary ensembles for the random problem; as the parameters approach the deter-

ministic problem's turning points, the random stationary ensembles are no longer well defined. This explains the lack of random solutions closer to the turning points in both diagrams, especially Figure 3b. In this case, the random stationary processes are no longer continuous in the parameter, and we can expect polynomial approximations to perform poorly; some have proposed remedies involving enrichment with discontinuous functions.¹⁷

Limit-Cycle Calculations

To perform limit-cycle computations, we set $B = 22$, $\beta = 3$, and designate Da to be a uniformly distributed random variable in $(0.083, 0.084)$. From deterministic analysis, we know that the CSTR system of Equation 10 exhibits limit-cycle solutions when $0.082 < Da < 0.085$. We select our Poincaré surface as the hyperplane (in this case, the line) of $x_1 = 0.9$. The numerical results show that $\langle x_2 \rangle = 5.3376$ with standard deviation $\sigma_{x_2} = 0.0075$, and the period has mean value $\langle T \rangle = 1.2284$ and a standard deviation $\sigma_T = 0.0032$.

Figure 4a shows a correlation between the x_2 value ($x_2(\omega)$) and the first return time ($T(\omega)$) for the fixed point of the coarse Poincaré map with uniformly distributed random $Da(\omega) \in (0.083, 0.084)$. Figure 4b plots several realizations of the periodic orbit; the time axis is normalized by $T(\omega)$.

Figure 5 presents the random limit cycle as $\langle x_1 \rangle$ versus error bars of $x_2(\omega)$. The error-bar clusters denote where the detailed MC computations occur, and projective integration takes place in the intervals between the clusters.

In principle, our equation-free approach combines the simplicity (and inherent embarrassing parallelism) of MC simulations with the power and convergence of nonsampling gPC representations. Equation-free “wrappers” have helped enable a wide variety of numerical tasks, from integration and fixed-point computation (illustrated here) to continuation, stability analysis, control, and optimization.^{1,2} We believe that our approach's nonintrusiveness could lower the “activation barrier” in developing and implementing gPC-based codes, thus facilitating UQ computations in engineering practice.

Current research directions include an extension of the equation-free UQ approach to spatially distributed uncertain problems and to cases in which the fine-scale simulator is atomistic or stochastic. Linking the approach with data analy-

sis techniques for the selection of appropriate macroscopic observables is also a promising research direction.

Acknowledgments

The US Air Force Office of Scientific Research, US Department of Energy, DARPA, the Army Research Office, the Office of Naval Research, and a US National Science Foundation/Information Technology Research grant partially supported this work.

References

1. I.G. Kevrekidis, C.W. Gear, and G. Hummer, "Equation-Free: The Computer-Assisted Analysis of Complex, Multiscale Systems," *Am. Inst. Chemical Engineers J.*, vol. 50, no. 7, 2004, pp. 1346–1354.
2. I.G. Kevrekidis et al., "Equation-Free Coarse-Grained Multiscale Computation: Enabling Microscopic Simulators to Perform System-Level Analysis," *Comm. Mathematical Sciences*, vol. 1, no. 4, 2003, pp. 715–762.
3. C. Theodoropoulos, Y. Qian, and I.G. Kevrekidis, "Coarse Stability and Bifurcation Analysis using Time Steppers: A Reaction-Diffusion Example," *Proc. Nat'l Academy Sciences*, vol. 97, Nat'l Academy Sciences, 2000, pp. 9840–9843.
4. C.T. Kelley, I.G. Kevrekidis, and Q. Liang, "Newton-Krylov Solvers for Time-Steppers," to be published in *SIAM J. Applied Dynamic Systems*, 2005; http://arxiv.org/PS_cache/math/pdf/0404/0404374.pdf.
5. C.W. Gear and I.G. Kevrekidis, "Projective Methods for Stiff Differential Equations: Problems with Gaps in Their Eigenvalue Spectrum," *SIAM J. Scientific Computing*, vol. 24, no. 4, 2003, pp. 1091–1106.
6. C.W. Gear, J. Li, and I.G. Kevrekidis, "The Gap-Tooth Method in Particle Simulations," *Physics Letters A*, vol. 316, nos. 3 and 4, 2003, pp. 190–195.
7. J. Li et al., "Deciding the Nature of the Coarse Integration through Microscopic Simulations: The Baby-Bathwater Scheme," *SIAM J. Multiscale Modeling and Simulation*, vol. 1, no. 3, 2003, pp. 391–407.
8. A. Makeev, D. Maroudas, and I.G. Kevrekidis, "Coarse Stability and Bifurcation Analysis using Stochastic Simulators: Kinetic Monte Carlo Examples," *J. Chemical Physics*, vol. 116, no. 23, 2002, pp. 10083–10091.
9. A. Makeev et al., "Coarse Bifurcation Analysis of Kinetic Monte Carlo Simulations: A Lattice-Gas Model with Lateral Interactions," *J. Chemical Physics*, vol. 117, no. 18, 2002, pp. 8229–8240.
10. O. Runborg, C. Theodoropoulos, and I.G. Kevrekidis, "Effective Bifurcation Analysis: A Time-Stepper-Based Approach," *Nonlinearity*, vol. 15, no. 2, 2002, pp. 491–511.
11. D. Xiu and I.G. Kevrekidis, "Equation-Free Multiscale Method for Unsteady Random Diffusion," to be published in *SIAM J. Multiscale Modeling and Simulation*, 2005.
12. C. Desceliers, R. Ghanem, and C. Soize, "Maximum Likelihood Estimation of Stochastic Chaos Representations from Experimental Data," to be published in *Int'l J. Numerical Methods in Eng.*, 2005.
13. D. Xiu and G.E. Karniadakis, "The Wiener-Askey Polynomial Chaos for Stochastic Differential Equations," *SIAM J. Scientific Computing*, vol. 24, no. 2, 2002, pp. 619–644.
14. C.W. Gear and I.G. Kevrekidis, "Telescopic Projective Methods for Parabolic Differential Equations," *J. Computational Physics*, vol. 187, no. 1, 2003, pp. 95–109.
15. R. Rico-Martinez, C.W. Gear, and I.G. Kevrekidis, "Coarse Pro-

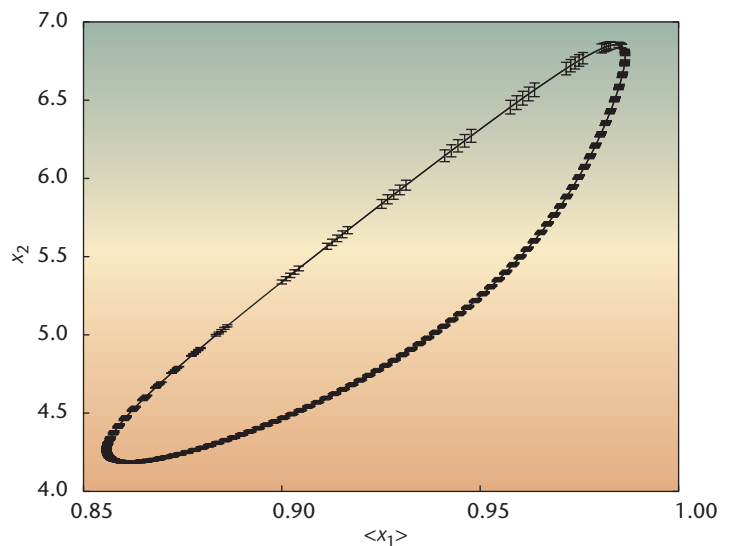


Figure 5. Oscillations under uncertainty. Phase portrait of the stochastic limit-cycle solution for Equation 10 with $B = 22$, $\beta = 3$, and a uniformly distributed random $Da \sim (0.083, 0.084)$.

jective kMC Integration: Forward/Reverse Initial and Boundary Value Problems," *J. Computational Physics*, vol. 196, no. 2, 2004, pp. 474–489.

16. A. Uppal, W.H. Ray, and A.B. Poore, "On the Dynamic Behavior of Continuous Stirred-Tank Reactors," *Chemical Eng. Science*, vol. 29, no. 3, 1974, pp. 967–985.
17. O. Le Maître et al., "Uncertainty Propagation using Wiener-Haar Expansions," *J. Computational Physics*, vol. 197, no. 1, 2004, pp. 28–57.

Dongbin Xiu is a postdoc research associate in the Division of Applied Mathematics at Brown University. His research interests are in scientific computation, uncertainty quantification, and multiscale modeling. Xiu has a PhD in applied mathematics from Brown University. Contact him at xiu@dam.brown.edu.

Roger Ghanem is a professor in the departments of aerospace and mechanical engineering and civil engineering at the University of Southern California. His research interests include stochastic modeling, computational stochastic mechanics, and multiscale modeling and analysis. Ghanem has an MCE and a PhD from Rice University. Contact him at ghanem@usc.edu.

Ioannis G. Kevrekidis is a professor of chemical engineering and of applied and computational mathematics at Princeton University (where he is also an associate faculty member in the mathematics department). His research interests are in the development and application of equation-free computation. He has an MA in mathematics and a PhD in chemical engineering from the University of Minnesota. Contact him at yannis@princeton.edu.